Structural Engineering and Mechanics, Vol. 42, No. 2 (2012) 247-267
DOI: http://dx.doi.org/10.12989/sem.2012.42.2.247

Prediction of seismic displacements in gravity retaining walls based on limit analysis approach

Mohammad Mojallal[a] and Ali Ghanbari*

Faculty of Engineering, Tarbiat Moallem University, No. 49 Mofatteh Ave., Tehran, I.R. Iran

(Received June 19, 2011, Revised February 28, 2012, Accepted March 20, 2012)

Abstract. Calculating the displacements of retaining walls under seismic loads is a crucial part in optimum design of these structures and unfortunately the techniques based on active seismic pressure are not sufficient alone for an appropriate design of the wall. Using limit analysis concepts, the seismic displacements of retaining walls are studied in present research. In this regard, applying limit analysis method and upper bound theorem, a new procedure is proposed for calculating the yield acceleration, critical angle of failure wedge, and permanent displacements of retaining walls in seismic conditions for two failure mechanisms, namely sliding and sliding-rotational modes. Also, the effect of internal friction angle of soil, the friction angle between wall and soil, maximum acceleration of the earthquake and height of the wall all in the magnitude of seismic displacements has been investigated by the suggested method. Two sets of ground acceleration records related to near-field and far-field domains are employed in analyses and eventually the results obtained from the suggested method are compared with those from other techniques.

Keywords: limit analysis; retaining walls; seismic displacement; yield acceleration

1. Introduction

In order to consider the economics of design and also mitigation of damage due to big earthquakes, knowing the behavior and seismic design of retaining walls is of significant importance. Analytical methods such as Mononobe-Okabe (1929, 1924) for calculation of active earth pressure provide advantageous information about the seismic loads applied to the wall, however the functionality of retaining walls after earthquakes is to a great extent dependent upon their deformations during the quake; simply because the induced active horizontal pressure behind the wall is a function of displacements and also direction of the wall's movement (Wu and Prakash 2001). Although large displacements can be acceptable for some walls but the other ones might encounter failure due to even small deformations. Therefore the analyses resulting in permanent deformations of retaining walls provide a better index of the wall's performance. Various methods have been proposed for determination of the permanent deformations of retaining walls, a brief description of which is presented here.

*Corresponding author, Associate Professor, E-mail: Ghanbari@tmu.ac.ir
[a]E-mail: mohammad.mojallal@yahoo.com

Newmark (1965) assumed the failure wedge as a rigid body ready to slide emplaced on the sliding surface. He calculated the horizontal seismic acceleration for the seismic stability of the slope given the safety factor of one. Then by two successive integration of the difference between accelerometer and yield acceleration, he was able to calculate the permanent displacements of the failure wedge. Richards and Elms (1979) proposed a simple technique based on the sliding block of Newmak for dynamic design of rigid retaining walls. The studies of Prakash and Wu (1996) show that calculated displacements by Richards and Elms (1979) underestimate the real values.

Using finite element method, Nadim (1982), Nadim and Whitman (1983) studied the displacements in retaining walls. Based on their studies, the seismic pressure applied to the wall can be 30% greater than the active earth pressure in static conditions. Also, if the ratio of the main frequency of ground motion to the frequency of backfill is greater than 0.3 then the resonance effect in the backfill plays an important role in permanent displacements of the wall (Wu and Prakash 2001). Whitman and Liao (1985) identified the errors of modeling approach proposed by Richards and Elms (1979). Using the results of sliding block analyses in 14 ground motions reported by Wong (1982), they noticed that the average permanent displacements have a normal logarithmic distribution pattern.

Among the other mathematical models for determination of walls' displacements, the models proposed by Rafnsson (1991), Rafnsson and Prakash (1994), Wu (1999) can be mentioned. Considering a system with two degrees of freedom and modeling the soil as a series of springs, Wu (1999) calculated both sliding and rotational displacements of retaining walls and verified his work by comparing the results with the experimental data reported by Zeng (1998) obtained from centrifuge tests. Huang (2006) studied the seismic displacements of two common bridge abutments in Taiwan by pseudo-static approach based on the multi-wedge theory and the sliding block theory of Newmark. In his analysis, the input ground acceleration was selected from the new and old design codes of Taiwan and displacements were calculated under four different ground acceleration records with and without consideration of the vertical acceleration. According to his research, the calculated seismic displacements for cantilever abutments were in the recommended range by design codes but in the case of gravity abutments it was more than allowable values. He also concluded that the presence of fill in front of the abutments has an important effect on reduction of seismic displacements.

Michalowski (2007) calculated the non-recoverable displacements of soil slopes during seismic triggers by the kinematic approach of limit analysis. A hodograph system was used to demonstrate the acceleration distribution in the structure for better understanding of the analysis. He concluded that in the soils where non-associated flow rule applied, the failure acceleration was smaller than soils with associated flow rule. Huang *et al.* (2009) employed a multi-wedge pseudo-static method to determine the seismic displacements of common walls from a series of shaking table experiments and the analytical method of Newmark (1965) based on the sliding block. Their results showed that the ratio of horizontal displacements of the wall to the height of the wall varied from 2 to 5% which covers a common range of displacements up to extensive failures. Eventually, they suggested the maximum seismic displacements of retaining walls in cohesionless soils be considered about 5% of the height of wall.

Based on limit equilibrium technique, Trandafir *et a*l. (2009) estimated the sliding failure and rotational failure displacements for retaining walls. They also calculated the rotational failure displacements for reinforced embankments. According to their studies, the vertical and horizontal seismic displacements in the crest of reinforced embankments were about 12% and 32% smaller

than vertical and horizontal seismic displacements of the crest of failure wedge behind a retaining wall, respectively.

Regarding the previous researchers did not calculate the seismic displacements of retaining walls based on limit analysis method; present study suggests a new procedure for calculation of seismic displacements based on kinematic limit analysis using upper bound theorem. In the proposed method, besides with calculating the seismic displacements, the angle of failure wedge is also determined under earthquake conditions for which the angle of dilation and associated flow rule (Normality Rule) are both considered in the behavior of soil.

2. Limit analysis

Finding analytical solutions is practically difficult for many engineering problems. Finn (1967), Chen (1975), Chen and Liu (1990) discussed purely analytical limit analysis solutions for some geotechnical problems (Drund *et al.* 2006). Limit analysis is a technique for stability assessments based on two theorems that make it possible to find upper and lower bound solutions for unknown quantities, such as the critical height of a slope and bearing capacity of foundations. Alternatively, material parameters can be estimated to maintain the stability of a given structure in a loading condition (Michalowski 1998). Lower and upper bound estimates of the collapse load factor can be obtained by both analytical and computational methods. In the case of lower bound solutions, statically admissible stress fields have to be assumed, whereas in the case of upper bound solutions, a kinematically admissible velocity fields must be assumed. In the latter case, this can be done by establishing a failure mechanism.

The lower bound theorem in its general form was independently established by Feinberg (1948) and proved by Hill (1948) by applying the principle of maximum plastic work to a finite volume of perfectly plastic material. A more complete statement of both lower and upper bound theorems and their proof was presented by Hill (1951) three years later. Drucker *et al*. (1952) first noted that the stress state remains constant at plastic collapse and threfore proved that the lower and upper bound theorems of limit analysis are also valid for elastic-plastic materials (Yu 2006).

The material involved in the analysis obeyed a convex yield condition, such as Mohr-coulomb criterion

$$f(\sigma_{ij}) = (\sigma_x + \sigma_y)\sin\phi - \sqrt{(\sigma_x - \sigma_y)^2 + 4\tau_{xy}^2} + 2c\cos\phi = 0 \tag{1}$$

where c and ϕ are the cohesion and internal friction angle of soil, respectively. Plastic deformations are governed by the normality (or associative) flow rule as follows

$$\dot{\varepsilon}_{ij}^{p} = \lambda \frac{\partial f(\sigma_{ij})}{\partial \sigma_{ij}} \qquad \begin{array}{ll} \lambda \geq 0 & \text{if } f = 0 \\ \lambda = 0 & \text{if } f < 0 \end{array} \tag{2}$$

where λ is a positive scalar multiplier, $f(\sigma_{ij})$ is the yield criterion, and $\dot{\varepsilon}_{ij}^{p}$ and σ_{ij} are the plastic strain rate and the stress tensor, respectively.

The upper bound theorem, which uses a rigid perfectly plastic soil model, states that the internal energy dissipated by any kinematically admissible velocity field can be equated to the work done by external loads**,** and so enables a strict upper bound on the actual solution to be deduced. The lowest possible upper bound solution is sought with an optimization scheme by trying various possible

kinematically admissible fracture surfaces. A kinematically admissible velocity field is the one that satisfies compatibility, a plastic flow rule and the velocity boundary conditions (Yang 2007). It is useful to write this theorem in a mathematical form as

$$\int \sigma_{ij}^{k} \dot{\varepsilon}_{ij}^{k} dV \geq \int_{S} T_i V_i dS + \int_{V} X_i V_i^{k} dV \tag{3}$$

In this equation, the left-hand side is the rate of the internal work or energy dissipation and in the right hand side the first term shows the unknown distributed load on boundary, S, and the second term shows the work rate of the given distributed forces per unit volume such as weight or inertial forces. Distributed loads on boundary S moving with velocity V_i (kinematic boundary condition) and distributed forces per unit volume are in the kinematically admissible velocity field V_i^k. σ_{ij}^k is the stress state which is in agreement with selected mechanism (satisfies the yield condition where plastic deformation occurs) (Michalowski 2007). The strain rate $\dot{\varepsilon}_{ij}^k$ represents any set of strains or deformations compatible with real or virtual displacement rate V_i or V_i^k of the points of the applications of the external forces T_i or the points of displacements corresponding to the body forces X_i (Chen 1975).

In recent years, several studies have been devoted to study the seismic stability of slopes and retaining walls (Michalowski 1998, You and Michalowski 1999, Sadrekarimi *et al.* 2008, Anastasopoulos *et al*. 2010, Gursoy and Durmus 2009, Haciefendioglu *et al*. 2010, Kim *et al.* 2008, Cocco *et al*. 2010).

3. Suggested formulation for calculating the permanent displacements

The proposed formulation in this research is based on kinematic limit analysis and upper bound theorem. The assumptions are as follows:

1. The failure wedge has been considered as a single planar block.
2. The Newmark sliding block method is used to estimate the seismic displacements.
3. The backfill is dry and cohesionless with no inclination and it follows the associated flow rule.
4. The retaining wall is considered as a rigid gravity wall which can tolerate sliding and rotational movements.

3.1 Calculation of critical failure angle in seismic conditions

A retaining wall with the height of H having a horizontal backfill with an internal friction angle of ϕ is considered. Internal friction angles of δ and ϕ_b between the wall and soil are taken into account, along the wall and in the foundation, respectively. The failure wedge is assumed as rigid and the Mohr-Coulomb failure criterion and associated flow rule are assumed to be valid. Inertial force of earthquake has been applied to both wall and soil in pseudo-static condition under horizontal and vertical accelerations of k_h and k_v, respectively.

In order to calculate the active pressure on the wall and determination of critical failure angle, the applied forces to the failure wedge and kinematic boundary conditions are considered as shown in Fig. 1. In this figure, V and V_0 are velocity vectors of the failure wedge and retaining wall, respectively, and V_1 is the relative velocity between the wall and failure wedge.

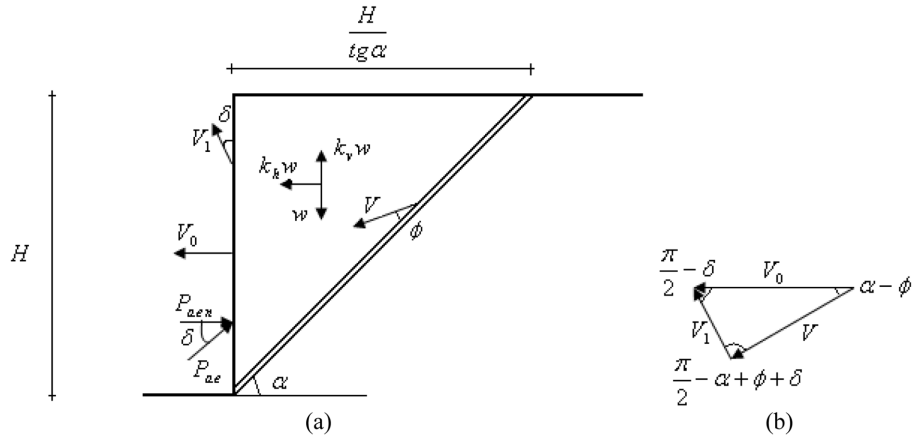

Fig. 1 (a) Applied forces to the wall, (b) Hodograph of velocities

Based on associated flow rule, the sliding vector, V, makes the angle of ϕ with the failure surface and the sliding vector, V_1, makes the angle of δ with the direction of wall and soil, assuming $\delta = 2/3\phi$. The rate of internal work or dissipated energy (D) is determined as follows

$$D = \frac{cH}{\sin\alpha} V\cos\phi \tag{4}$$

where c is the cohesion of soil and assume to be zero.

Based on the upper bound theorem of limit analysis and Eq. (3), the rate of work for external force is equal to

$$\int x_i V_i^k dv = (1-k_v)\dot{W}_1 + k_h w V\cos(\alpha-\phi) + P_{aen} V_0 \cos(\pi) \tag{5}$$

$$\dot{W}_1 = wV\sin(\alpha-\phi) \tag{6}$$

Where X_i is the force in the unit of volume, $\dot{W}_1$ is the work rate of the gravity forces of the wedge and P_{aen} is the active force perpendicular to the wall.

Regarding Fig. 1(b), where the velocity vectors in the initial failure wedge and their relations are depicted, the correlation between V and V_0 is determined as follows

$$V_0 = V\frac{\cos(\alpha-\phi-\delta)}{\cos\delta} \tag{7}$$

Substituting Eqs. (4) to (7) into Eq. (3) we obtain

$$\frac{cHV\cos\phi}{\sin\alpha} \geq (1-k_v)wV\sin(\alpha-\phi) + k_h wV\cos(\alpha-\phi) - P_{aen}V\frac{\cos(\alpha-\phi-\delta)}{\cos\delta} \tag{8}$$

Regarding the absence of surface load (T_i = 0), the first term in Eq. (3) has been eliminated making the left hand side of Eq. (8) equal to the second term in Eq. (3).

The weight of failure wedge, w, is equal to

$$w = \frac{H^2}{2tg\alpha}\gamma_s \tag{9}$$

To calculate an upper bound for the active force in Eq. (8), the inequality is changed to equality. Substituting Eq. (9) in Eq. (8), it can be written

$$P_{aen} = \frac{\left[(1-k_v)\frac{H^2}{2tg\alpha}\gamma_s \sin(\alpha-\phi) + k_h \frac{H^2}{2tg\alpha}\gamma_s \cos(\alpha-\phi) - \frac{cH\cos\phi}{\sin\alpha}\right]\cos\delta}{\cos(\alpha-\phi-\delta)} \tag{10}$$

Assuming $c = 0$ and simplifying the Eq. (10), the active force is determined as follows

$$P_{ae} = \frac{\gamma_s H^2[(1-k_v)\sin(\alpha-\phi) + k_h\cos(\alpha-\phi)]}{2tg\alpha\cos(\alpha-\phi-\delta)} \tag{11}$$

where P_{ae} is the active force making the angle of δ with the wall and P_{aen} is the active force, perpendicular to the wall.

In common analyses of the slides, inclination angle, α, is usually given. In order to obtain the best estimation (i.e., least upper bound), the active force as a function of α needs to be maximized, hence

$$\frac{\partial P_{ae}}{\partial \alpha} = 0 \tag{12}$$

Since determination of α based on other parameters is mathematically difficult, the solution of Eq. (12) is proposed for δ as a function of α and ϕ.

$$tg\delta = \frac{tg(\alpha-\phi) - [C_{E1} + C_{E2}]}{1 + tg(\alpha-\phi)[C_{E1} + C_{E2}]} \tag{13}$$

$$C_{E1} = -\cot(\alpha - \phi + \xi) \tag{14}$$

$$C_{E2} = \frac{1 + tg^2\alpha}{tg\alpha} \tag{15}$$

$$\xi = tg^{-1}\left(\frac{k_h}{1-k_v}\right) \tag{16}$$

Eq. (13) has been solved by trial and error for different values of α resulting in the critical failure wedge of the retaining wall.

3.2 Permanent displacements of the wall

The first step in estimating the permanent displacements of the wall by upper bound theorem is calculating the k_y. A gravity wall with granular backfill and height of H is shown in Fig. 2(a).

In order to calculate the failure acceleration, two blocks have been considered. The first block is the failure wedge behind the wall and the second block is the gravity wall itself. According to associated flow rule, the velocity vector makes a certain angle with the failure lines in kinematic boundary conditions.

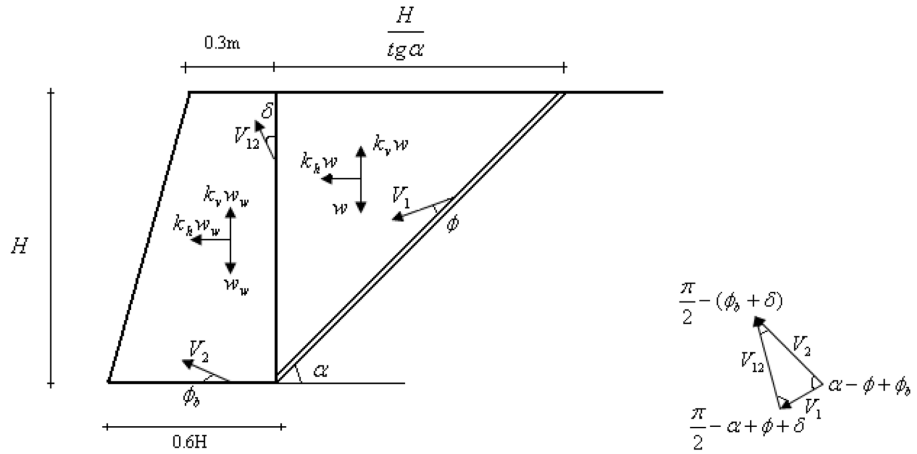

Fig. 2 Single-block initial failure mechanism: (a) initial velocities, (b) Hodograph of velocity

Mentioned angle is equal to the internal friction angle of soil (ϕ) along the failure wedge. This angle along the wall and soil, and the failure line in the foundation is equal to δ and ϕ_b, respectively. The relation between velocities is illustrated in Fig. 2(b). In Fig. 2, V_1 and V_2 are velocity vectors of failure wedge and retaining wall, respectively and V_{12} is the relative velocity between the wall and failure wedge.

Considering Fig. 2(a) and Eq. (3), the rate of external work and rate of internal work (dissipation of energy), are determined as follows

$$D \geq (1-k_v)\dot{W} + k_h w V_1 \cos(\alpha - \phi) + (1-k_v)\dot{W}_w + k_h w_w V_2 \cos\phi_b \tag{17}$$

$\dot{W}$ and $\dot{W}_w$ are the rates of work done by gravity force in the soil block and in the wall block, respectively. These two rates are calculated by Eqs. (18) and (19)

$$\dot{W} = w V_1 \sin(\alpha - \phi) \tag{18}$$

$$\dot{W} = -w_w V_2 \sin\phi_b \tag{19}$$

Rate of work done by the surface force is equal to zero in Eq. (3). The right hand side of the inequality (17) is equal to the rate of work done by volumetric forces. Assuming at the time of failure, the ground motion acceleration is reached the yield acceleration ($k_y = k_h$); it can be written

$$D = (1-k_v)[\dot{W} + \dot{W}_w] + k_y[w V_1 \cos(\alpha - \phi) + w_w V_2 \cos\phi_b] \tag{20}$$

Regarding the Fig. 2(b), following relation can be concluded

$$V_1 = V_2 \frac{\cos(\phi_b + \delta)}{\cos(\alpha - \phi - \delta)} = V_2 \cdot B \tag{21}$$

Substituting Eq. (21) into Eq. (20), the vertical component of yield acceleration is calculated as

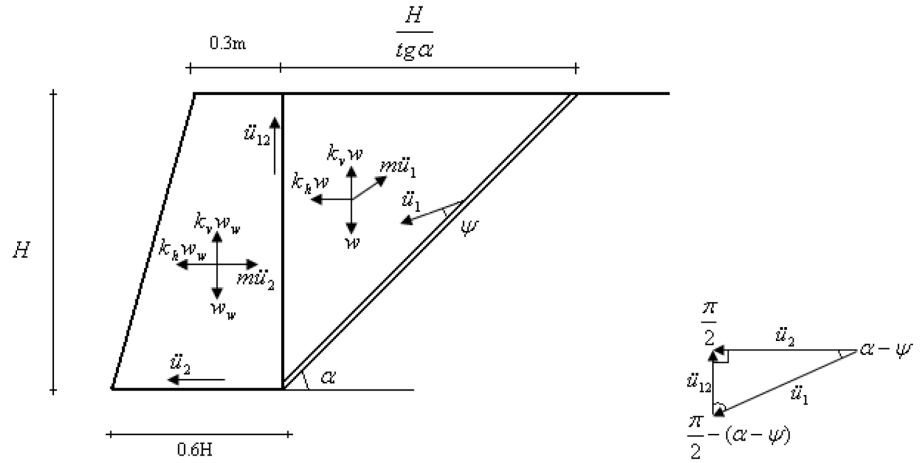

Fig. 3 Displacement mechanisms of the wall (a) Mechanism I, (b) Hodograph of acceleration for the mechanism I

$$k_y = \frac{D-(1-k_v)[\dot{W}+\dot{W}_w]}{wB\cos(\alpha-\phi)+w_w\cos\phi_b} = \frac{D-(1-k_v)[wB\sin(\alpha-\phi)-w_w\sin\phi_b]}{wB\cos(\alpha-\phi)+w_w\cos\phi_b} \tag{22}$$

where D is the rate of internal work done by cohesion of soil. w_w and w are the weights of wall and failure wedge, respectively. w is defined in Eq. (9) and w_w equals to

$$w_w = \left(\frac{0.3+0.6H}{2}\right)H\gamma_c \tag{23}$$

In order to predict permanent displacement of retaining wall two mechanisms proposed. In mechanism I, with assumption of wall's foundation be incompressible, the dilatancy angle becomes zero. This assumption made because in granular soils, dilatancy is typically less than that predicted with associative law (Michalowski 2007). However, in mechanism II without considering this assumption, the dilatancy angle becomes equal to friction angle. However if the soil does not obey associative flow rule completely, or contains water or cohesion, this approach should be modified and other parameters should be considered in the formula. Moreover, because in medium density backfill, the value of δ is between $\frac{1}{2}\phi$ and $\frac{2}{3}\phi$ (Das 1983), in these calculations δ is being equal to $\frac{2}{3}\phi$.

When the earthquake acceleration exceeds the yield acceleration of structure ($k > k_y$), two mechanisms might occur. In mechanism I, as shown in Fig. 3(a), the wall only experiences the sliding failure and moves with the acceleration of $\ddot{u}_2$. Soil block also moves with the acceleration of $\ddot{u}_1$ in this mechanism. In the second mechanism (II) the wall experiences both sliding and rotational displacements (Fig. 4(a)) and thus the wall and soil block move with accelerations of $\ddot{u}_2$ and $\ddot{u}_1$ respectively.

The relation between the acceleration vectors in mechanisms I and II are demonstrated in Figs. 3(b) and 4(b), respectively. Mentioned mechanisms do not act like the incipient process which leads to inequality in Eq. (3) and consequently $\ddot{u}_1$ and $\ddot{u}_2$ are real accelerations and the real velocities would be obtained by one integration from these accelerations. A second integration does lead to determination of displacements parallel to the principal accelerations for retaining walls and

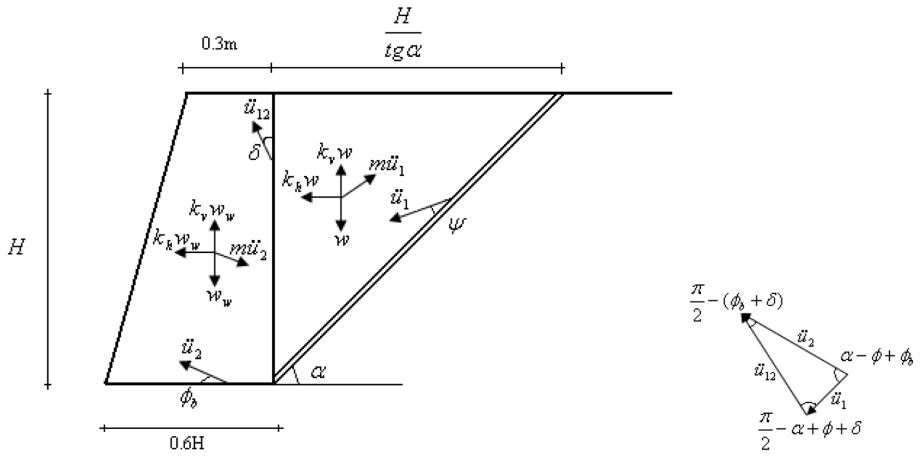

Fig. 4 Displacement mechanisms of the wall (a) Mechanism II, (b) Hodograph of acceleration for the mechanism II

soil block.

The sliding process occurs along the failure surfaces during the seismic quakes. These failure surfaces are brought about when the earthquake acceleration reaches the yield acceleration of structure. Sliding surfaces in this analysis are considered as a thin layer of soil (shear band). Considering the backfill soil satisfies the associated flow rule and dilation is not zero, in both mechanisms the acceleration vector $\ddot{u}_1$ and consequently direction of sliding surface make the angles of $\psi = \phi$ with the failure surface in which ψ is the dilation angle of soil.

In mechanism I assuming the sliding failure, acceleration vectors $\ddot{u}_2$ and $\ddot{u}_{12}$ and therefore the direction of sliding are parallel to the failure surface. In mechanism II assuming of rotational and sliding displacement, the acceleration velocities $\ddot{u}_2$ and $\ddot{u}_{12}$ and consequently direction of sliding will make the angles of $\psi_b = \phi_b$ and $\psi = \delta$ with the failure surface, respectively. The rate of balance of work of all forces applied to both blocks, can be written as follows

For mechanism I

$$D + m_w \ddot{u}_2 V_2 \cos\phi_b + (m\ddot{u}_1) V_1 \cos(\phi - \psi) = (1 - k_v)[\dot{W} + \dot{W}_w] + k[w V_1 \cos(\alpha - \phi) + w_w V_2 \cos\phi_b]$$
$$k > k_y \tag{24}$$

For mechanism II

$$D + m_w \ddot{u}_2 V_2 \cos(\phi_b - \psi_b) + m\ddot{u}_1 V_1 \cos(\phi - \psi) = (1 - k_v)[\dot{W} + \dot{W}_w] + k[w V_1 \cos(\alpha - \phi) + w_w V_2 \cos\phi_b]$$
$$k > k_y \tag{25}$$

where $\dot{W}$ and $\dot{W}_w$ are obtained from Eqs. (18) and (19).

Inertial forces in two blocks are caused by accelerations ($\ddot{u}_1$ and $\ddot{u}_2$) and their directions are opposite to the direction of acceleration vectors hence their rate of work would be negative. But in the Eqs. (24) and (25) they appear with positive sign in the left side. Regarding Figs. 3(b) and 4(b) it can be written

$$\ddot{u}_1 = \frac{\ddot{u}_2}{\cos(\alpha-\phi)} \Rightarrow \ddot{u}_1 = B'\ddot{u}_2 \quad \text{(For mechanism I)} \tag{26}$$

$$\ddot{u}_1 = \frac{\cos(\phi_b+\delta)}{\cos(\alpha-\phi-\delta)}\ddot{u}_2 \Rightarrow \ddot{u}_1 = B\ddot{u}_2 \quad \text{(For mechanism II)} \tag{27}$$

Substituting Eq. (20) in Eqs. (24) and (25) it can be written:
For mechanism I

$$m_w\ddot{u}_2V_2\cos\phi_b + m\ddot{u}_1V_1\cos(\phi-\psi) = (k-k_y)[wV_1\cos(\alpha-\phi) + w_wV_2\cos\phi_b] \tag{28}$$

For mechanism II

$$m_w\ddot{u}_2V_2\cos(\phi_b-\psi_b) + m\ddot{u}_1V_1\cos(\phi-\psi) = (k-k_y)[wV_1\cos(\alpha-\phi) + w_wV_2\cos\phi_b] \tag{29}$$

Substituting Eqs. (21) and (26) into Eq. (28) and also Eqs. (21) and (27) into Eq. (29) and rearranging the terms, acceleration of wall block in the foundation is obtained as:
For mechanism I

$$\ddot{u}_2 = (k-k_y)g\frac{[mB\cos(\alpha-\phi) + m_w\cos\phi_b]}{[m_w\cos\phi_b + mBB'\cos(\phi-\psi)]} = g(k-k_y)C \tag{30}$$

For mechanism II

$$\ddot{u}_2 = (k-k_y)g\frac{[mB\cos(\alpha-\phi) + m_w\cos\phi_b]}{[m_w\cos(\phi_b-\psi_b) + mB^2\cos(\phi-\psi)]} = g(k-k_y)C' \tag{31}$$

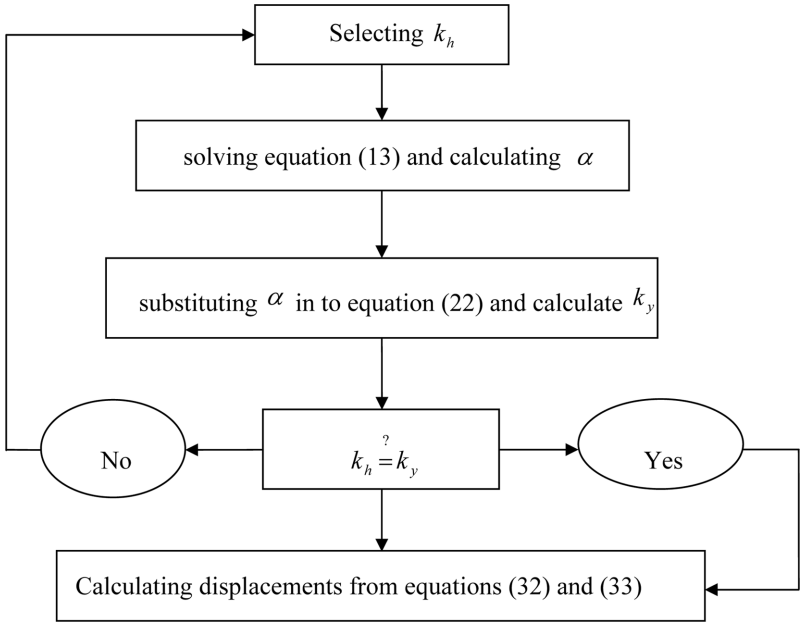

Fig. 5 Algorithm used to determine the yield acceleration

where C and C' are constants dependent on the geometry of mechanism and material properties. Finally by two successive integration from Eqs. (30) and (31), sliding displacement in mechanism (I) and sliding and rotational displacement of the wall in mechanism II are calculated as:

For mechanism I

$$u_2 = C\int\int g(k-k_y)dtdt \qquad V>0 \tag{32}$$

For mechanism II

$$u_2 = C'\int\int g(k-k_y)dtdt \qquad V>0 \tag{33}$$

Since k_y is a function of α and the critical angle of failure (α) is also dependent on k_h, Eqs. (13) and (22) are solved simultaneously by trial and error based on the algorithm shown in Fig. 5.

4. Obtained results from the suggested method

In this section using the obtained formulation from section 3 and considering the mechanism I (sliding displacement of retaining wall), the effect of soil and wall properties and also the maximum acceleration of earthquake on permanent displacements of retaining walls are investigated.

4.1 Effect of maximum earthquake acceleration coefficient on permanent displacements of retaining walls

A retaining wall with the height of H = 10 m and specific weight of concrete $\gamma_c = 24\frac{kN}{m^3}$ is considered. A horizontal backfill (i.e., zero inclination angle or $\beta = 0$) with the height of 10 m and internal friction angle of $\phi = 30^o$ and specific weight of soil $\gamma_s = 20\frac{kN}{m^3}$ and also $\delta = \frac{2}{3}\phi$ is assumed. Internal friction angle between the soil and foundation of wall is considered as $\phi_b = 0.86\phi$ and the backfill is considered as cohesionless soil (c = 0). Since the frequency components of different accelerometers are not the same, in order to investigate the effect of maximum earthquake acceleration coefficient, the accelerometer related to Northridge-1994

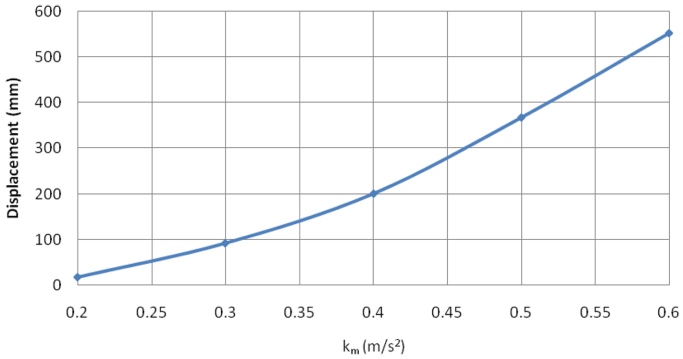

Fig. 6 Effect of the maximum acceleration coefficient of earthquake on the permanent displacements of retaining wall

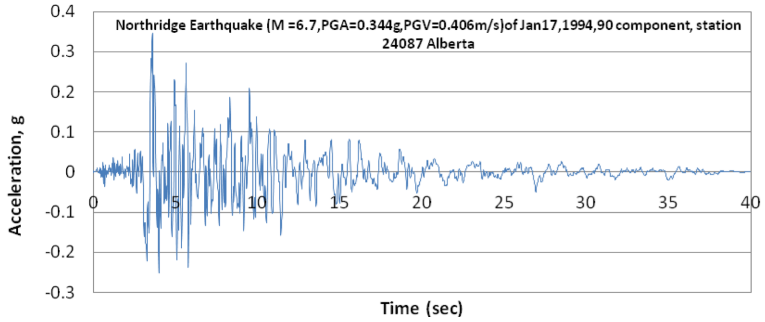

Fig. 7 Record of Northridge earthquake

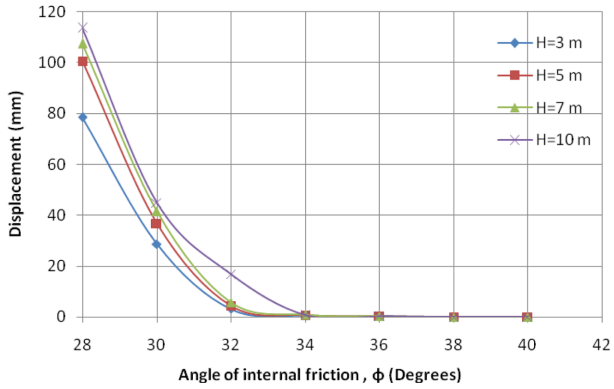

Fig. 8 Effect of internal friction angle of backfill on permanent displacements of retaining wall

earthquake has been employed instead of using several records with different PGAs. This record is scaled for different maximum accelerations (Fig. 7).

Using Eq. (13) and the algorithm shown in Fig. 5, k_y and C are obtained for the mentioned wall and backfill as 0.103 and 0.9422, respectively (coefficient in Eq. (30)). Fig. 6 demonstrates the increasing trend of seismic displacements of the wall as k_m increases.

4.2 The effect of backfill's internal friction angle on displacements of retaining wall

Fig. 8 shows the permanent displacements of retaining wall for different internal friction angles. These variations are studied for walls with different heights. As can be observed from Fig. 8, for a known internal friction angle, displacements increase as the height of wall increases. These results are obtained for the record shown in Fig. 7.

4.3 The effect of height of the wall on seismic displacements of the retaining wall

It is anticipated that for a certain ϕ and under a constant accelerometer, as the height of the wall increases, permanent displacements also increase which is consistent with the curve obtained from calculations in part 3 of this paper. In order to investigate the effect of internal friction angle of the foundation (ϕ_b), the displacements have been estimated under the Northridge-1994 accelerometer for $\phi = \phi_b$ and $\phi_b = 0.86\phi$. Obtained results are shown in Figs. 9 and 10.

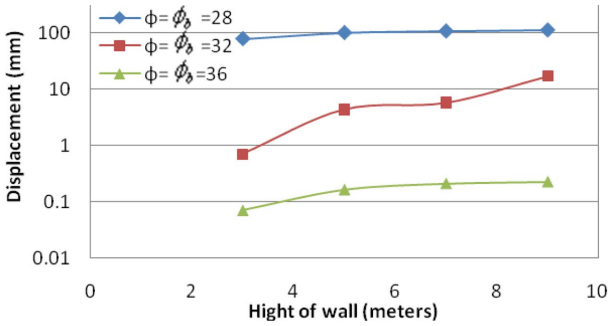

Fig. 9 The effect of height of the wall on displacements of retaining wall $\phi = \phi_b$

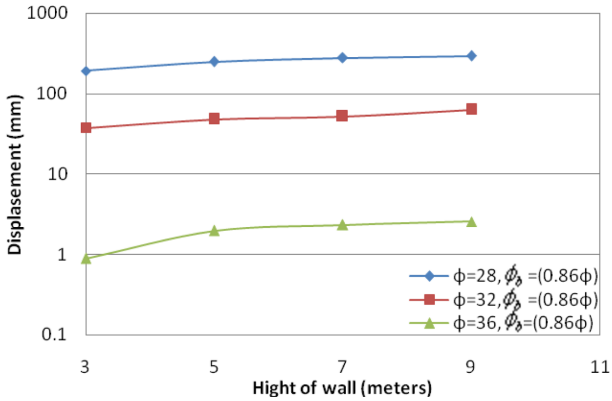

Fig. 10 The effect of height of the wall on displacements of retaining wall $\phi_b = 0.86\phi$

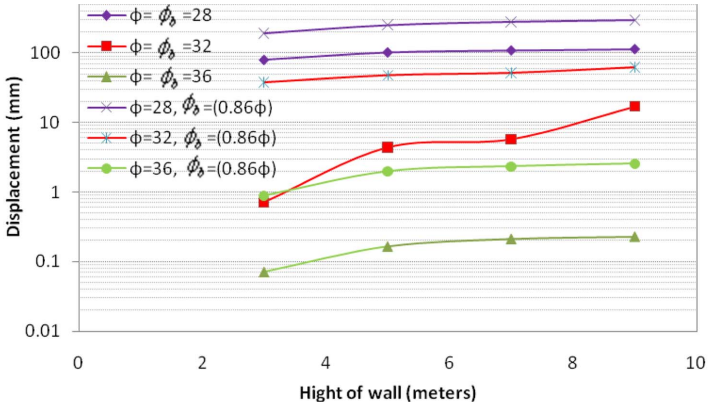

Fig. 11 Effect of ϕ_b on permanent displacements of the wall

According to these figures, permanent displacements of the wall have been increased with decrease in ϕ_b. The displacements are shown in logarithmic vertical axis in all three plots. Fig. 11 illustrates the effect of ϕ_b on permanent displacements of the retaining wall.

4.4 Investigating the permanent displacements of wall for far-field and near-field domain earthquakes

For the analyses of this section, 7 records from far-field domain have been compared with 5 records from near-field domain which maximum accelerations are scaled for the values of 0.2, 0.3 and 0.4 g. The retaining wall and backfill are assumed similar to section 4.1. These records are shown in Figs. 12 and 13, respectively.

According to the results obtained from suggested method (mechanism I) the effects of these records on displacements of retaining wall are investigated in Figs. 14 and 15, respectively. In all of these records, the displacements increase with increase in maximum acceleration**.**

In Fig. 16, a comparison has been made between displacements of retaining wall under far-field and near-field records. As can be observed in the Fig. 16, near-field domain records induce greater permanent displacements in the retaining wall compared with far-field domain records with the same maximum acceleration.

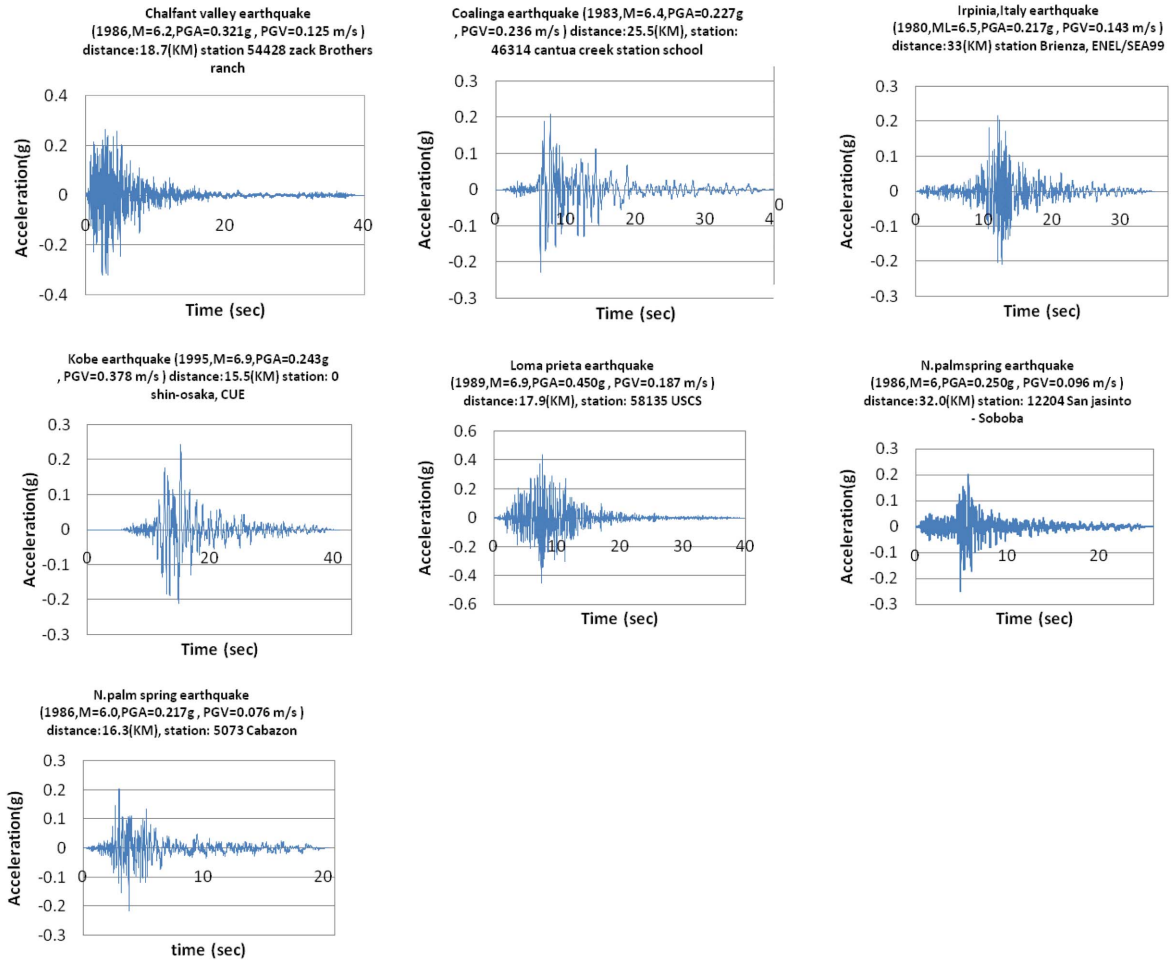

Fig. 12 Far field records

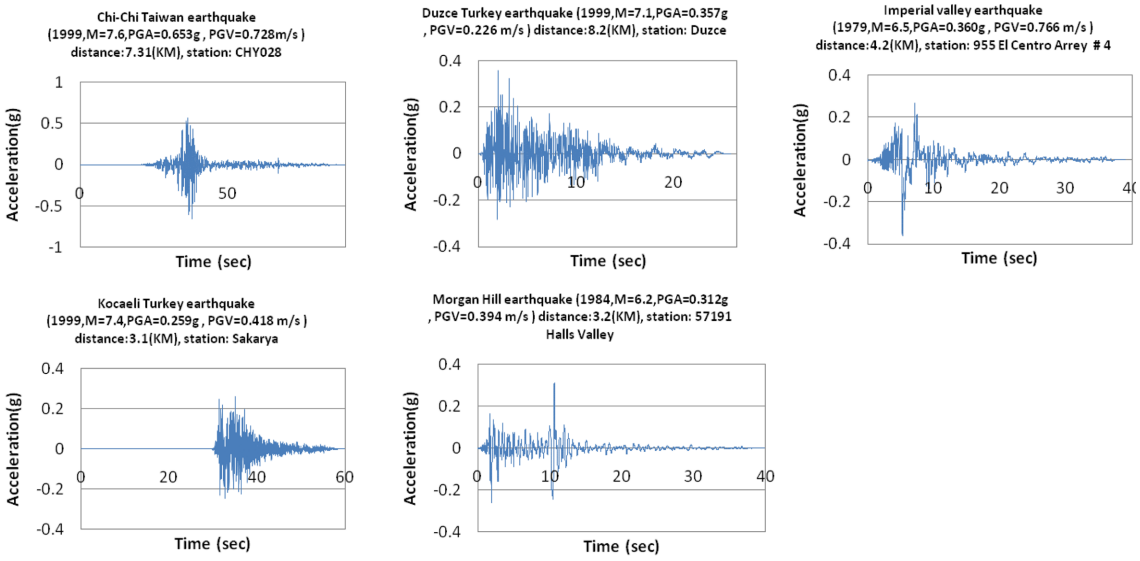

Fig. 13 Near field records

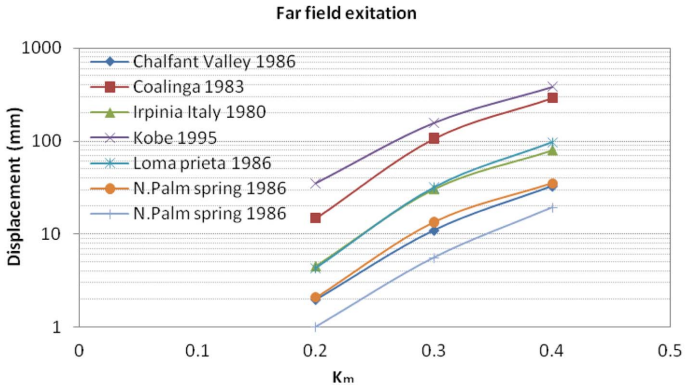

Fig. 14 Permanent displacement of retaining wall under far-field domain earthquakes

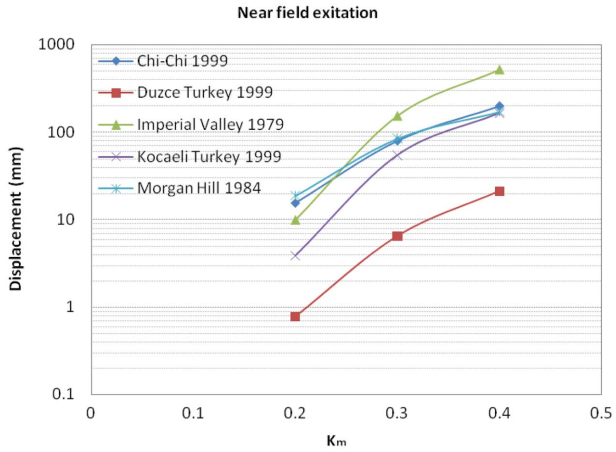

Fig. 15 Permanent displacements of retaining wall under near-field domain earthquakes

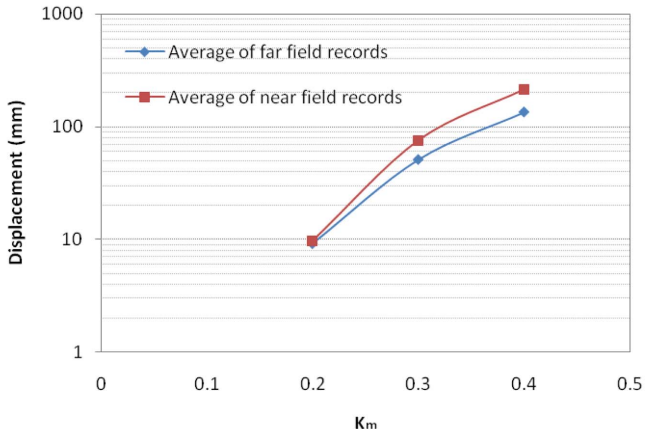

Fig. 16 The effect of record type on permanent displacements of retaining wall

5. Comparison of results with those reported by other researchers

For the mentioned retaining wall in section 4.1, the critical failure angle (α) has been calculated using the suggested method (Eq. (13)). The results from present formulation compare very well with those reported by Zarrabi-Kashani (1979) as can be observed in Table 1. Table 2 shows a comparison between k_y calculated from current method and k_y obtained from Michalowski (2007) method and there is a good agreement between them.

Table 1 Comparison between critical angle of failure obtained from suggested method and Zarrabi-Kashani (1979) method Specific weight of backfill

k_h	Height of the wall H (m)	α Zarrabi-Kashani (1979)	α Proposed method	Specific weight of backfill γ_s (kN/m)	Friction angle of granular backfill ϕ (Degrees)	Specific weight of concrete γ_c (kN/m^3)	Inclination angle of backfill β (Degrees)
0.1	10	50.53	50.5	20	30	24	0
0.2	10	46.10	45.8	20	32	24	0
0.25	10	44.78	44.2	20	34	24	0
0.3	10	43.51	42.6	20	36	24	0

Table 2 Comparison between k_y obtained in this paper with the k_y calculated by Michalowski (2007) method

k_m Northridge earthquake	Height of the wall H (m)	Inclination angle of backfill β (Degrees)	Specific weight of concrete γ_c (kN/m^3)	Friction angle of granular backfill ϕ (Degrees)	Specific weight of backfill γ_s (kN/m^3)	k_y proposed method	k_y Michalowski (2007)
0.344 g	3	0	24	30	20	0.181	0.180
	5	0	24	30	20	0.169	0.169
	7	0	24	30	20	0.163	0.163
	10	0	24	30	20	0.159	0.159

Table 3 Properties of the two models used in analyses

Model	δ (Degrees)	Height of the wall H (m)	Inclination angle of backfill β (Degrees)	Specific weight of concrete γ_c (kN/m^3)	Friction angle of granular backfill ϕ (Degrees)	Specific weight of backfill γ_s (kN/m^3)	w_w (kN /m)	ϕ_b (Degrees)
1	15	8.1	0	24	30	19	669.16	25.8
2	22	4	0	24	33	21.6	130.08	23.3

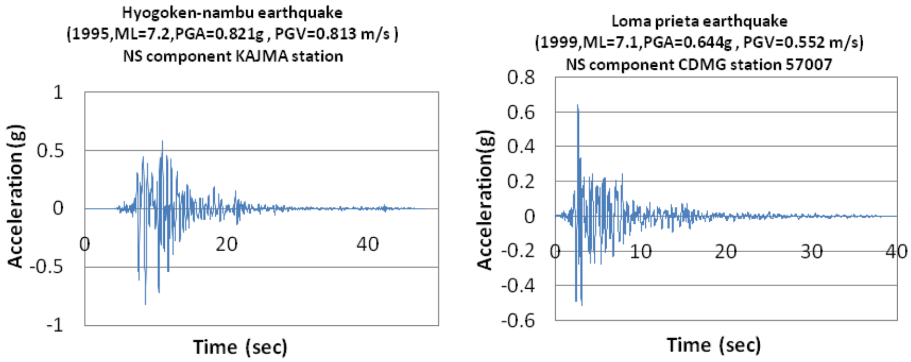

Fig. 17 Records of accelerations used in analysis of model 1

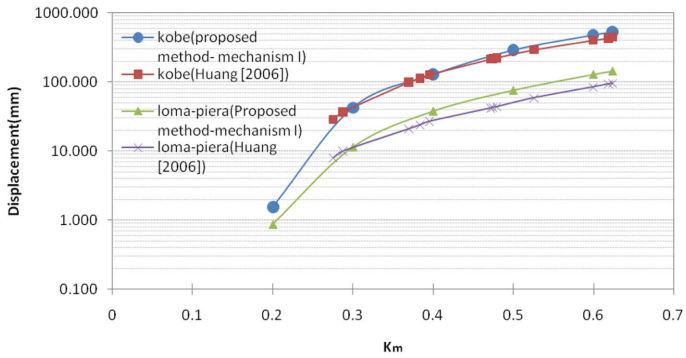

Fig. 18 Comparison of wall's displacements from the first model obtained by the suggested method under mechanism I and the method proposed by Huang (2006)

In order to compare the displacements calculated from suggested method with those from other researchers two models have been considered of whose properties are noted in Table 3. These two models have been analyzed and permanent displacements of retaining wall under different accelerometers (Figs. 17 and 7) are determined. Obtained results in the first model only include sliding displacements of the wall and in the second model both sliding and sliding-rotational displacements are included.

Permanent displacements of the retaining wall from the first model calculated by suggested method under mechanism I are compared with the method proposed by Huang (2006) in Fig. 18.

Table 4 Comparison of permanent displacements of the retaining wall obtained by current method and the studies of other researchers

	Proposed method (Sliding-Rotational)	Wu (1999) (Sliding-Rotational)	Proposed method (Sliding)	Wu (1999) (Sliding)	Richards and Elms (1979)	Whitman and Liao (1985)
k_y	0.097	-	0.097	-	0.155	0.1
Displacement (m)	0.167	0.166	0.150	0.062	0.095	0.118

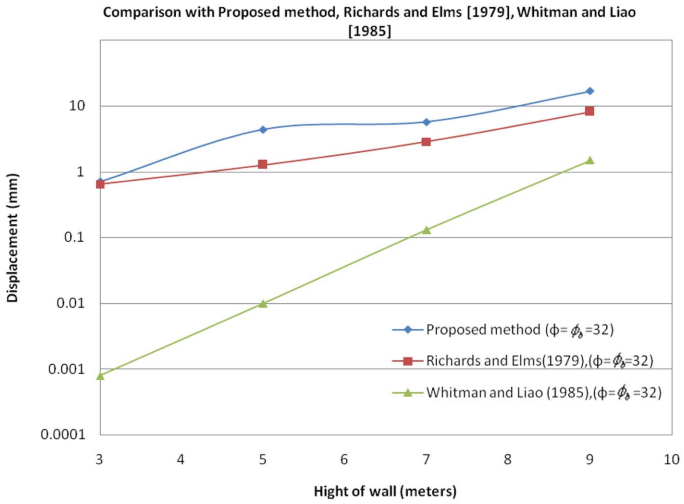

Fig. 19 Analysis of displacements calculated by the suggested method and the other methods for retaining walls with different heights

This model has been analyzed under accelerometers whose maximum accelerations are scaled for the values of 0.2 g, 0.3 g, 0.4 g, 0.5 g, 0.6 g and 0.624 as shown in Fig. 17 and permanent displacements of the retaining wall are compared. The results of present method are a little greater than those reported by Huang (2006) in both cases.

Table 4 shows the sliding and sliding- rotational displacements of model 2 estimated by the suggested method and those obtained using work principles by Wu (1999), Richards and Elms (1979), Whitman and Liao (1985) under the Norhridge-1994 earthquake. Obtained displacements from the current formulation are greater than those from other studies. In other words, present values can be considered as an upper bound for those reported by other researchers.

Fig. 19 shows the effect of height on permanent displacements of retaining wall under the Northridge-1994 earthquake. Obtained results from the suggested method considering mechanism I are compared in Fig. 19 with those reported by Richards and Elms (1979), Whitman and Liao (1985) methods. In this study $\phi = \phi_b = 32$, $\delta = 2/3\phi$, $\gamma_s = 20$ kN/m^3 and $\gamma_c = 24$ kN/m^3.

Even here obtained displacements from the suggested method are greater than the other results or in other words, present results are an upper bound for those reported by other researchers.

6. Conclusions

In this paper using the upper bound theorem of limit analysis and presenting a new formulation, permanent displacements, and critical failure wedge and yield acceleration of retaining walls are determined. In this method, the soil properties such as dilatancy angle, associated flow rule and geometry of model are all taken into account in calculating the displacements of retaining wall. Two mechanisms are considered in determination of permanent displacements of retaining wall. The mechanism I calculates the sliding displacements and mechanism II calculates the sliding-rotational displacements.

The effect of height of wall, internal friction angle of soil (ϕ), friction angle between soil and wall (ϕ_b, δ) and maximum acceleration applied to the structure a_{max} in permanent displacements of retaining wall are also considered. Eventually, permanent displacements of the retaining wall estimated from the suggested method based on mechanisms I and II are compared with the results reported by other researchers.

Obtained results from suggested formulation reveal that by increase in the height of wall, decrease in ϕ and ϕ_b, increase in a_{max} and reduction in the distance of structure from the fault (applying the near-field domain records) permanent displacements of retaining wall increase. Also permanent displacements in mechanism II are greater in comparison with mechanism I. The yield acceleration obtained from current method using the presented algorithm led to very close values as reported by Michalowski (2007) which shows the precision of suggested formulation. The critical failure angle calculated from present method resulted in values close to those reported by Zarrabi-Kashani (1979).

Comparison of permanent displacements calculated based on suggested method and for mechanism I, with the proposed method by Huang (2006) shows that the trend of variations in these methods are the same. However the suggested method is an upper bound for that proposed by Huang (2006). Also the obtained results from current formulation and for the mechanism I are an upper bound for sliding displacements calculated by Richards and Elms (1979), Whitman and Liao (1985) and Wu (1999). Calculated displacement from mechanism II is very close to the sliding-rotational displacement reported by Wu (1999).

It can be concluded that present formulation which is based on the upper bound theorem of limit analysis is of great capability in calculating the permanent displacements of retaining walls.

References

Anastasopoulos, I., Georgarakos, T., Georgiannou, V., Drosos, V. and Kourkoulis, R. (2010), "Seismic performance of bar-mat reinforced-soil retaining wall: Shaking table testing versus numerical analysis with modified kinematic hardening constitutive model", *Soil Dyn. Earthq. Eng.*, **30**(10), 1089-1105.

Chen, W.F. (1975), *Limit Analysis and Soil Plasticity*, Elsevier, Amsterdam.

Chen, W.F. and Liu, X.L. (1990), *Limit Analysis in Soil Mechanics*, Elsevier, Amsterdam.

Cocco, L., Suarez, L.E. and Matheu, E.E. (2010), "Development of a nonlinear seismic response capacity spectrum method for intake towers of dams", *Struct. Eng. Mech.*, **36**(3), 321-341.

Das, B.M. (2009), *Principles of Geotechnical Engineering*, Seventh Edition, Cangage Learning.

Durand, A.F., Vargas, Jr E.A. and Vaz, L.E. (2006), "Applications of numerical limit analysis (NLA) to stability problems of rock and soil masses", *Int. J. Rock Mech. Mining Sci.*, **43**, 408-425.

Drucker, D.C., Prager, W. and Greenmberg, H.G. (1952), "Etended limit design theorems for continuous media",

Quart. J. Mech. Appl. Math., **9**, 381-389.
Feinberg, S.M. (1948), *The Principle of Limiting Stresses*, Prnkl Mat Mech, 12. (In Russian)
Finn, W.D.L. (1967), "Application of limit plasticity in soil mechanics", *J. Soil Mech. Found. Div.-ASCE*, **93**(5), 101-120.
Gursoy, S. and Durmus, A. (2009), "Investigation of linear and nonlinear of behaviours of reinforced concrete cantilever retaining walls according to the earthquake loads considering", *Struct. Eng. Mech.*, **31**(1), 75-91.
Haciefendioglu, K., Bayraktar, A. and Turker, T. (2010), "Seismic response of concrete gravity dam-ice covered reservoir-foundation interaction systems", *Struct. Eng. Mech.*, **36**(4), 499-511.
Hill, R. (1948), "A variational principle of maximum plastic work in classical plasticity", *Quart. J. Mech. Appl. Math.*, **1**, 18-28.
Hill, R. (1951), "On the state of stress in a plastic-rigid body at the yield point", *Philos. Mag.*, **42**, 868-875.
Huang, C.C. (2006), "Seismic displacement analysis of free-standing highway bridge abutment", *J. GeoEng.*, **1**(1), 29-39.
Huang, C.C., Wu, S.H. and Wu, H.J. (2009), "Seismic displacement criterion for soil retaining walls based on soil strength mobilization", *J. Geotech. Geoenvir. Eng.-ASCE* , **135**(1), 76-82.
Kim, T.H., Kim, Y.J. and Shin, H.M. (2008), "Seismic performance assessment of reinforced concrete bridge piers supported by laminated rubber bearings", *Struct. Eng. Mech.*, **29**(3), 259-278.
Michalowski, R.L. (1998), "Limit analysis in stability calculations of reinforced soil structures", *Geotext. Geomembrain.*, **16**(6), 311-331.
Michalowski, R.L. (1998), "Soil reinforcement for seismic design of geotechnical structures", *Comput. Geotech.*, **23**(1-2), 1-17.
Michalowski, R.L. (2007), "Displacement of multiblock geotechnical structures subjected to seismic excitation", *J. Geotech. Geoenvir. Eng.-ASCE*, **133**(11), 1432-1439.
Mononobe, N. and Matsuo, H. (1929), "On the determination of earth pressures during earthquakes", *Proceedings of the World Engineering Congress*, Tokyo, Japan.
Nadim, F. (1982), "A numerical model for evaluation of seismic behavior of gravity retaining walls", ScD Thesis, Research report R82-33, Department of Civil Engineering, Massachusetts Institute of Technology.
Nadim, F. and Whitman, R.V. (1983), "Seismically induced movement of retaining walls", *J. Geotech. Eng.-ASCE*, **109**(7), 915-931.
Newmark, N.M. (1965), "Effects of earthquakes on dams and embankments", *Geotechnique*, **15**(2), 139-159.
Okabe, S. (1924), "General theory on earth pressure and seismic stability of retaining wall and dam", *J. Japan Soc. Civil Eng.*, **10**(6), 1277-1323.
Rafnsson, E.A. (1991), "Displacement based design of rigid retaining walls subjected to dynamic loads considering soil nonlinearity", PhD Dissertation, University of Missouri-Rolla.
Rafnsson, E.A. and Prakash, S. (1994), "Displacement based a seismic design of retaining walls", *Proceedings of XIII International Conference of Soil Mechanics and Foundation Engineering*, New Delhi.
Richards, R. and Elms, D.G. (1979), "Seismic behavior of gravity retaining walls", *J. Geotech. Eng. Div.*, **105**(4), 449-464.
Sadrekarimi, A., Ghalandarzadeh, A. and Sadrekarimi, J. (2008), "Static and dynamic behavior of hunchbacked gravity quay walls", *Soil Dyn. Earthq. Eng.*, **28**(2), 99-117.
Trandafir, A.C., Kamaja, T. and Sidle, R.C. (2009), "Earthquake-induced displacement of gravity retaining walls and anchor-reinforced slopes", *Soil Dyn. Earthq. Eng.*, **29**, 428-437.
Whitman, R.V. and Liao, S. (1985), "Seismic design of retaining walls", Miscellaneous paper GL-85-1, Department of the Army, US Army Corps Engineers, Washington, DC.
Wong, C.P. (1982), "Seismic analysis and improved seismic design procedure for gravity retaining walls", M.S. Thesis, Department of Civil Engineering, Massachusetts Institute of Technology.
Wu, Y. and Prakash, S. (1996), "On seismic displacements of rigid retaining walls, Analysis and design of retaining structures against earthquakes", *J. Geotech. Geoenvir. Eng.,* **60**, 21-37.
Wu, Y. (1999), "Displacement-based analysis and design of rigid retaining walls during earthquake", PhD Dissertation, Univ. of Missouri-Rolla.
Wu, Y. and Prakash, S. (2001), "Seismic displacement of rigid retaining walls - state of the art", *Proceedings of the Fourth International Conference on Recent Advances in Geotechnical Earthquake Engineering and Soil*

*Dynamic*s, San Diego, California, March.
Yang, X.L. (2007), "Upper bound limits analysis of active earth pressure with different fracture surface and nonlinear yield criterion", *Theo. Appl. Frac. Mech.*, **47**(1), 46-56.
You, L. and Michalowski, R.L. (1999), Displacement charts for slopes subjected to seismic loads", *Comput. Geotech.*, **25**(1), 45-55.
Yu, H.S. (2006), *Plasticity and Geotechnics*, Springer Science + Business Media LLC.
Zarrabi-Kashani, K. (1979), "Sliding of gravity retaining wall during earthquakes considering vertical accelerations and changing inclination of failure surface", M.S. Thesis, Department of Civil Engineering, Massachusetts Institute of Technology.
Zeng, X. (1998), "Seismic response of gravity quay walls I: centrifuge modeling", *J. Geotech. Geoenvir. Eng., ASCE*, **124**(5), 406-417.